

Partial Field Opening and Current Sheet Formation in the Disk Magnetosphere

Dmitri A. Uzdensky

Institute for Theoretical Physics, University of California

Santa Barbara, CA 93106

`uzdensky@itp.ucsb.edu`

February 4, 2002

ABSTRACT

In this paper I analyze the process of formation of thin current structures in the magnetosphere of a conducting accretion disk in response to the field-line twisting brought about by the rotation of the disk relative to the central star. I consider an axisymmetric force-free magnetically-linked star-disk configuration and investigate the expansion of the poloidal field lines and partial field-line opening caused by the differential rotation between the star and a nonuniformly-rotating disk. I present a simple analytical model that describes the asymptotic behavior of the field in the strong-expansion limit. I demonstrate the existence of a finite (of order one radian) critical twist angle, beyond which the poloidal field starts inflating very rapidly. If the relative star-disk twist is enhanced locally, in some finite part of the disk (which may be the case for a Keplerian disk that extends inward significantly closer to the central star than the corotation radius), then, as the twist is increased by a finite amount, the field approaches a partially-open configuration, with some field lines going out to infinity. Simultaneous with this partial field opening, a very thin, radially extended current layer forms, thus laying out a way towards reconnection in the disk magnetosphere. Reconnection, in turn, leads to a very interesting scenario for a quasi-periodic behavior of magnetically-linked star-disk systems with successive cycles of field inflation, opening, and reconnection.

Subject headings: accretion, accretion disks — magnetic fields — MHD — stars: magnetic fields

1. Introduction

Magnetic processes taking place in the magnetosphere above a thin accretion disk play an important role in establishing the structure of disk outflows (winds and jets), in regulating the accretion flow,

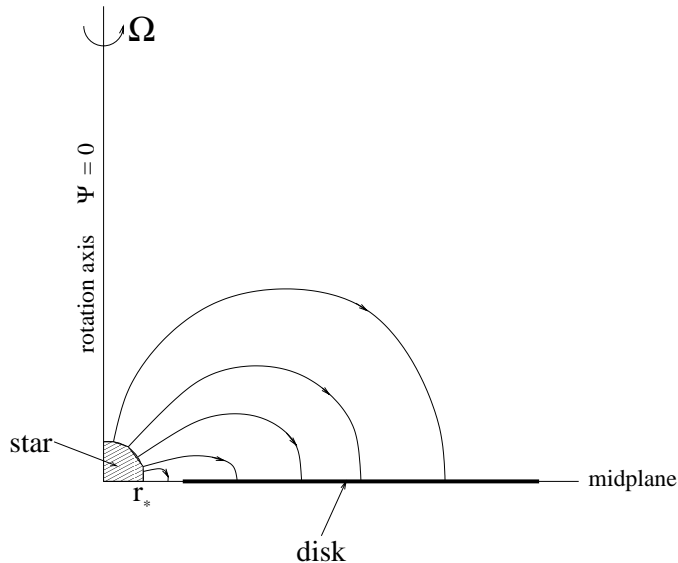


Fig. 1.— Axisymmetric magnetically-linked star-disk system.

and in angular momentum transfer. Of particular interest is the situation where there is a direct magnetic connection between the star and the disk (the so-called magnetically-linked star-disk system, see Fig. 1). This connection may lead to a direct angular momentum exchange between the disk and the star and is thus relevant for neutron star spin-up/spin-down events (Ghosh & Lamb 1978, 1979; Wang 1987; Lovelace et al. 1995). It is also important because it provides a mechanism for direct channeling of accretion flow onto the polar regions of the star (Bertout, Basri, & Bouvier 1988; Lamb 1989; Patterson 1994; Königl 1991).

The evolution and even the sole existence of such a configuration depends critically on the conducting properties of the disk, the star, and the overlying magnetosphere. This complex physical problem can be studied on various time scales; one should start, however, with the shortest relevant time scale, namely, the rotation period. On this time scale both the central star and the disk can usually be approximated by ideal conductors (with the exception of the case when the central object is a black hole), and so can the low-density magnetosphere (or corona) that lies above the disk. In this case there is no steady state because the differential rotation between the disk and the star leads to continuous twisting of the field lines. The magnetic field in the magnetosphere responds to this differential rotation by rapid expansion driven by the increased toroidal field pressure. The field lines become elongated along a direction making a roughly 60° angle with the rotation axis. This expansion process has been studied in some detail in the framework of the force-free model.¹ In particular, semi-analytic self-similar models (van Ballegooijen 1994, hereafter

¹The validity of the force-free approximation in these systems is justified by the fact that, due to very low density in the magnetosphere, the Alfvén velocity there greatly exceeds both the sound speed and the rotation speed.

$n=0.5$

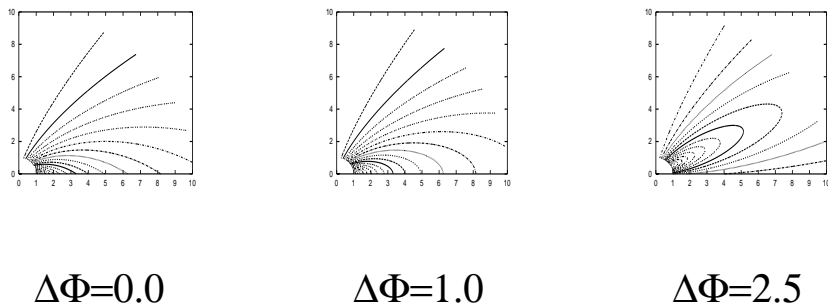


Fig. 2.— Field-line expansion caused by the relative rotation of the disk with respect to the star in the case of the $n = 0.5$ self-similar model, where $\Psi_{\text{disk}} \sim r^{-n}$ (This figure is taken from Uzdensky et al. 2002a).

VB94; Lynden-Bell & Boily 1994, hereafter LBB94; Uzdensky et al. 2002a) have shown that the field-line expansion leads to an effective opening of the field lines after a finite (a few radians) twist angle (see Fig. 2). This finite-time singularity has also been observed in numerically constructed non-self-similar sequences of force-free equilibria (Uzdensky et al. 2002a) and also in non-force-free full-MHD numerical simulations by Goodson et al. (1997, 1999). This process is essentially very similar to the process of finite-time field-line opening of a twisted coronal field studied extensively in solar physics (see, e.g., Barnes & Sturrock 1972; Low 1986; Roumeliotis et al. 1994; Mikić & Linker 1994; Wolfson 1995; Aly 1995). Thus, at present there is growing evidence that a finite-time opening of field lines in response to differential rotation is a generic feature of force-free magnetospheres of magnetically-linked star-disk systems.

It is, however, still not clear what happens after this opening. Basically, one can envision two possible outcomes: the field lines may either reconnect (across the separatrix between the two domains with the opposite direction of the radial field) and close back; or they may stay open indefinitely. In the first scenario (Aly & Kuijpers 1990, VB94, Goodson et al. 1997, 1999) some resistivity is present in the magnetosphere, and as a result, a small amount of flux gets immediately reconnected, leading to the formation of an X-point. As reconnection progresses, a toroidal plasmoid forms in the magnetosphere. This plasmoid contains most of the toroidal flux; it becomes completely detached from both the disk or the star and just floats away, presumably feeding a jet (Goodson et al. 1999). At the same time, the magnetic link between the star and the disk is reestablished, with the reconnected magnetic field lines being now twisted less than they were just before the reconnection event. The poloidal magnetic field tension then quickly contracts them back towards the star, and the system returns to its initial state. Thus, in this scenario the situation is manifestly time-dependent; the time evolution consists of periodic cycles of successive field line inflation due to the differential shearing, “effective” field-line opening, reconnection, and the relaxation of the

reconnected magnetic field to the initial state (of lesser magnetic stress), which completes the cycle.

In the second scenario, investigated by Lovelace et al. (1995), there is no reconnection and a true steady state is established, whereby the field is at least partially open and the magnetic link between the star and a significant part of the disk is permanently broken.

The fact that the above two scenarios differ so dramatically raises the level of urgency of identifying the conditions under which each of them can be realized. The main difference between these two pictures is that *magnetic reconnection* is allowed to take place in one but not in the other. Thus, as it often happens in astrophysics and space physics, the physics of magnetic reconnection plays a key role. This issue is by no means trivial and it is questionable whether it could be resolved even by a direct numerical simulation. Indeed, numerical simulations typically suffer from unrealistically large numerical resistivities that make it very easy for oppositely directed field lines to reconnect (as seems to be the case with the simulations by Goodson et al. 1999).

It is usually the case that in order to get efficient reconnection, a thin current sheet is needed. In the two-dimensional axisymmetric situation discussed here, a natural place where such a current sheet can arise as the system approaches the open-field state is the current concentration region between the two domains with oppositely directed radial magnetic field. While the field lines are still closed, the current is concentrated along the apex line $\theta = \theta_{\text{ap}}(\Psi)$.² As the field opens up, this apex line turns itself into the separatrix between two regions of oppositely directed, open (i.e., extending to infinity) field lines that comprise the open-field configuration. If one now considers such a configuration (where the field lines have already been opened), then one discovers that the formation of a current sheet is essentially unavoidable, at least as long as the force-free approximation is valid.³ Indeed, an *open* magnetic field is potential, it has no toroidal field. This is because all toroidal flux created by the initial twisting has escaped to infinity as the result of magnetic field expansion and opening. The field becomes predominantly radial everywhere, with B_r reversing across the separatrix $\theta = \theta_{\text{ap}}$. In the absence of the toroidal field B_ϕ at $\theta = \theta_{\text{ap}}$, the pressure balance across the separatrix cannot be maintained, and this leads to the collapse of the magnetic configuration to one with an infinitesimally thin current sheet; the two oppositely directed magnetic fields move toward each other, forming a thin current layer. Finally, the collapse is stopped when resistive (or other non-ideal) effects become important in the layer. Because the current density is tremendously increased, magnetic reconnection can occur.

²Here, $\theta_{\text{ap}}(\Psi)$ marks the angular position of the apex of an inflated field line (an apex is defined as the farthest from the central star point on a field line). Usually, θ_{ap} is close to 60° and depends only very weakly on the field line Ψ .

³As was pointed out by the referee of this paper, if a heated atmosphere is present above the disk, then, once the magnetic field opens up, the drop of magnetic intensity with distance may be fast enough for the disk wind far out to dominate and keep the field from reconnecting. The centrifugal wind could also hold the field open provided there is a lower, sufficiently heated atmosphere to feed that wind. This may be the implied reasoning behind the apparent neglect of the possibility of reconnection by Lovelace's et al. (1995).

It is important to realize, however, that, strictly speaking, as long as one has a force-free magnetic field with the field lines *closed*, one can never have a true, infinitesimally thin current sheet. Indeed, while the system is going through a sequence of equilibria of *closed* field lines, i.e., for $t < t_c$ (where t_c marks the moment time of field-line opening), there is always finite toroidal field, B_ϕ , present. This is because it is the toroidal flux that drives the expansion along $\theta = \theta_{\text{ap}}$, and in a force-free equilibrium its outward pressure balances against the poloidal field’s large curvature. Thus, in a closed force-free configuration the toroidal flux is kept in place by the poloidal field tension and prevents poloidal field lines from contracting back to a less-stressed state. At the same time, this toroidal field provides the pressure in the θ direction, which prevents the poloidal field collapse into a current sheet configuration.

One could ask, however, whether a current sheet can form *asymptotically*, that is, whether the sequence of force-free equilibria, which governs the system’s evolution, can asymptotically lead to stronger and stronger thinning of the current concentration region as one approaches the critical moment, so that the characteristic angular width of this region, $\Delta\theta$, goes to zero as $t \rightarrow t_c$. Note that this does not always happen. For example, in the self-similar force-free model for a uniformly rotating disk (VB94; Uzdensky et al. 2002a), where all magnetic quantities are power laws of r with fixed power-law indices, $\Delta\theta$ does not go to zero but approaches a finite value that depends solely on the flux distribution $\Psi_{\text{disk}}(r)$ on the disk surface. In particular, if $\Psi_{\text{disk}}(r) \sim r^{-n}$, then $\Delta\theta$ approaches a finite value of order a fraction of one radian if $n = O(1)$ (and is proportional to n in the limit $n \rightarrow 0$), as the critical moment t_c is approached.

Asymptotic current sheet formation was in fact observed in the self-similar model by LBB94 (in cylindrical geometry) and also in an essentially very similar work by Wolfson (1995) (in spherical geometry in the solar corona context). This is explained by the fact that the power law index n was forced to change during the evolution. In particular, in the cylindrical case considered by LBB94, all magnetic flux was required to go through the boundary at some small radius (compared with the radius under consideration). Therefore, for each value of the power exponent n , the resulting equilibrium corresponded to a member of the VB94 family of solutions in the limit of infinite expansion, $t \rightarrow t_c(n)$ (this limit was analyzed in detail by Uzdensky et al. 2002a). Since in the VB94 analysis $t_c(n)$ grows as $n \rightarrow 0$, the gradual increase of the twist angle with time meant that, when considering the LBB94 solutions, one were bound to obtain a sequence of solutions with ever diminishing values of n [determined from the condition $t_c(n) = t$]. That is, in the LBB94 sequence of solutions, n had to decrease and approached zero at some point, which lead to the reported thinning and formation of a current sheet. Related to this change of n was the fact that the field-line footpoints were allowed (and actually had) to move poloidally. If, instead, one insisted on having the footpoints tied firmly to the disk surface, then the flux distribution on this surface (which, in the self-similar model, must be a power law extending to arbitrary large radii) could not change, at least on the short, rotation-period time scale considered here. Then n and, hence, $\Delta\theta$ would both stay finite. Under these circumstances the prospects for magnetic reconnection to occur in a timely manner would be very slim, at least in the two-dimensional framework (see

Uzdensky et al. 2002b).

Thus, the transformation of the current concentration region into a true, infinitesimally-thin current sheet, even in the asymptotic sense, cannot, in general, be taken for granted.

The failure of the self-similar force-free model to provide a plausible current-sheet formation (and hence reconnection) scenario makes it increasingly important to try to understand the asymptotic current-sheet formation process in a more general situation where the self-similar model does not apply. In particular, it is interesting to ask whether (still within a force-free framework) the current-concentration region can become very thin, thus indicating a way towards forming a true current sheet. If such a thin current layer does form, what is its structure? In particular, what is the Ψ -profile of the angular width $\Delta\theta$ and how does it depend on the twist angle profile $\Delta\Phi(\Psi)$?

It is important to realize that in the self-similar model there is no special radial scale and hence all the field lines must open up simultaneously. In a general, non-self-similar situation, however, there is a possibility of a *partial field-line opening*,⁴ with the domain of open field lines being adjacent to that of closed field lines. As we shall discuss below, this can greatly facilitate the current-sheet formation process.

On the intuitive level, the basic idea of how a thin magnetic structure can form in the disk magnetosphere is simple. Imagine a *non-uniformly* rotating disk. In particular, consider a system on the brink of the partial field-line opening: let there be a field line Ψ_c such that, as the system approaches a certain critical time t_c , the field lines outside of Ψ_c (i.e., $\Psi < \Psi_c$) tend to open, while those inside stay closed.⁵ Now, if $\Delta\Omega(\Psi)$ [and hence the twist $\Delta\Phi(\Psi) = \Delta\Omega t$] is nonuniform, say, rising outward, then the degree of expansion of field lines will also be non-uniform. Indeed, two neighboring field lines $\Psi_1 = \Psi_c + \delta\Psi$ and $\Psi_2 = \Psi_c - \delta\Psi$ will have their footpoints close to each other, while their apexes $r_{\text{ap}}(\Psi_1)$ and $r_{\text{ap}}(\Psi_2)$ will be very far apart since $r_{\text{ap}}(\Psi_1)$ should stay finite whereas $r_{\text{ap}}(\Psi_2) \rightarrow \infty$ as $t \rightarrow t_c$. In other words, $d \log r_{\text{ap}}(\Psi) / d \log \Psi$ at $\Psi = \Psi_c$ will go to infinity as $t \rightarrow t_c$. As we shall show in this paper, a thinning of the apex region (i.e., current layer formation) is characteristic for a situation like this, which is consistent with the spirit of the studies by LBB94 and by Wolfson (1995) who both show that a current sheet forms asymptotically when $n \equiv d \log \Psi / d \log r \rightarrow 0$.

Thus, the main thrust of this paper is to demonstrate how twisting of field lines leads to the formation of thin current structures that asymptotically become thinner and thinner as the field approaches a partially-open state in finite time. In § 2 we present the basic geometry of the problem and a description of our model. In §§ 3–5 we discuss the three main components of the model:

⁴The importance of partial field-line opening in solar coronal processes has been recognized and emphasized by Low (1990) and by Wolfson & Low (1992), who suggested that a partially open field configuration may be energetically accessible even when a completely open configuration is not.

⁵We count poloidal magnetic flux Ψ from the outside inward, i.e., we set $\Psi(\pi/2, r \rightarrow \infty) \rightarrow 0$.

§ 3 focuses on the purely geometrical relationship between the twist angle of the field lines and the relative strength of the toroidal field, while §§ 4 and 5 describe our treatment of the θ – and the radial force balance equations, respectively. In § 6 we formulate and discuss the final set of differential equations describing the behavior of the angular thickness of the current concentration region. Also in that section we consider three specific examples: § 6.1 deals with the constant-twist case, § 6.2 investigates the behavior in the vicinity of the critical twist angle, and § 6.3 describes a numerical solution of our equations for the case of a locally-enhanced twist angle. We present our conclusions in § 7.

Finally, we note that although we consider this problem in the accretion disk context, our methods and the main findings can be directly applied in the solar corona context. In particular, we note that the differential-rotation-driven process of partial field-line opening (and the detachment of the toroidal plasmoid associated with it) is essentially very similar to a coronal mass ejection; in addition, the partially opened field configuration considered in this paper is similar to a coronal helmet streamer configuration (see, for example, Low 2001).

2. Description of the Model

In spherical coordinates (r, θ, ϕ) , the poloidal components of an axisymmetric magnetic field can be written in terms of the poloidal magnetic flux function Ψ as

$$B_r = \frac{1}{r^2 \sin \theta} \frac{\partial \Psi}{\partial \theta}, \quad (1)$$

$$B_\theta = -\frac{1}{r \sin \theta} \frac{\partial \Psi}{\partial r}. \quad (2)$$

In a force-free equilibrium the magnetic flux function satisfies the Grad–Shafranov equation,

$$\frac{\partial^2 \Psi}{\partial r^2} + \frac{\sin \theta}{r^2} \frac{\partial}{\partial \theta} \left(\frac{1}{\sin \theta} \frac{\partial \Psi}{\partial \theta} \right) = -F F'(\Psi), \quad (3)$$

where the *generating function*

$$F = B_\phi r \sin \theta \quad (4)$$

is $2/c$ times the total poloidal current flowing through the circle defined by $\phi \in [0, 2\pi]$ at fixed (r, θ) . Since in an axisymmetric equilibrium poloidal current must follow poloidal field lines, F is constant along the field lines, i.e., $F = F(\Psi)$.

Now, consider a configuration with the dipole-like field topology, and assume that the magnetic axis coincides with the rotation axes of both the disk and the star. We are interested in a situation where the system is approaching the point of field-line opening, so that the field lines are expanded very strongly along the direction of their apexes $\theta = \theta_{\text{ap}}$, so that $r_{\text{ap}}(\Psi) \gg r_0(\Psi)$ (where $r_{\text{ap}}(\Psi)$ and

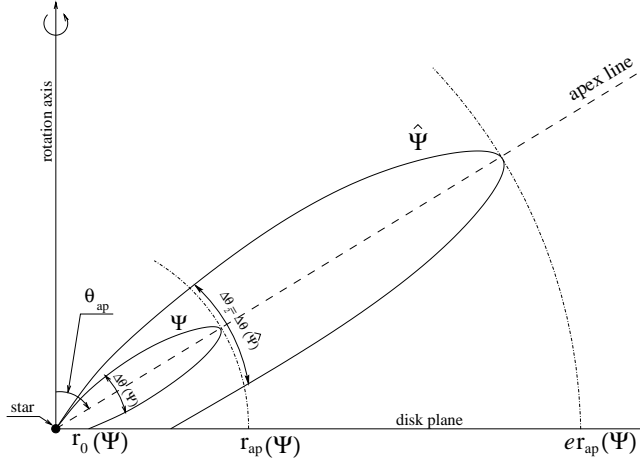


Fig. 3.— Geometry of the problem: strongly expanded field lines in the magnetosphere of a magnetically-linked star–disk system.

$r_0(\Psi)$ are the radial positions of the apex and the disk footpoint of field line Ψ ; see Fig. 3). In this asymptotic regime $\theta_{\text{ap}}(\Psi)$ should not change much from one field line to another. In the self-similar model, for example, $\theta_{\text{ap}}(\Psi)$ is, of course, exactly the same for all field lines and varies by only a few degrees as n changes from 0 to 1; and in the non-self-similar numerical model of Uzdensky et al. (2002a), $\theta_{\text{ap}}(\Psi)$ lies between 60 and 70°. In any case, the Ψ dependence of θ_{ap} is much weaker than that of the field line parameters r_{ap} and $\Delta\theta$ (the latter is defined immediately below); therefore, we shall neglect this dependence in our analysis and assume that the apex direction is the same for all field lines,

$$\theta_{\text{ap}}(\Psi) = \text{const.} \quad (5)$$

Next, for a given field line Ψ , let us define the angular width $\Delta\theta_1 = \Delta\theta(\Psi)$ of the region enveloped by this field line. For definiteness, we define $\Delta\theta(\Psi)$ in terms of the shape $r(\theta, \Psi)$ of the field line as

$$r\left(\Psi, \theta_{\text{ap}} + \frac{\Delta\theta(\Psi)}{2}\right) \equiv \frac{r_{\text{ap}}(\Psi)}{e} \simeq r\left(\Psi, \theta_{\text{ap}} - \frac{\Delta\theta(\Psi)}{2}\right), \quad (6)$$

where $e = 2.7183\dots$ is the base of the natural logarithm.

In addition to $\Delta\theta_1 = \Delta\theta(\Psi)$, we also define $\Delta\theta_2$ as $\Delta\theta_2(\Psi) \equiv \Delta\theta(\hat{\Psi})$, where $\hat{\Psi}$ is the field line with the apex radius $r_{\text{ap}}(\hat{\Psi})$ equal to e times $r_{\text{ap}}(\Psi)$ (see Fig. 3). The quantity $\Delta\theta_2(\Psi)$ can also serve as an estimate for the characteristic angular width [at a given $r = r_{\text{ap}}(\Psi)$] of the region where most of the toroidal flux, as well as most of the toroidal current, are concentrated.

We are interested in the situation where thin structures are about to form in the magnetosphere. Therefore, throughout this paper we shall systematically assume that

$$\Delta\theta(\Psi) \ll 1, \quad (7)$$

for all field lines Ψ under consideration.

Our main goal is to evaluate $\Delta\theta(\Psi)$ and to determine how it changes in response to an increased twist angle.

Our program has three main ingredients. First, there is a purely geometric constraint relating the twist angle $\Delta\Phi(\Psi)$ to the function $F(\Psi)$ and to the poloidal field B_θ . The other two ingredients are dynamic — they reflect the force-free magnetic force balance in two directions, across and along the apex line (the θ and the radial directions, respectively). Upon the completion of this program we shall obtain three equations relating three functions, $F(\Psi)$, $\Delta\theta(\Psi)$, and $r_{\text{ap}}(\Psi)$, to each other. This will allow us to investigate under what circumstances thin structures can form. We start with the geometric constraint.

3. The Twist Angle Constraint

The twist angle $\Delta\Phi(\Psi)$ of a field line is defined as the difference between the toroidal positions of the footpoints of this field line on the surface of the disk and that of the star. It can be written as

$$\Delta\Phi(\Psi) = F(\Psi)I(\Psi). \quad (8)$$

Here, the function $I(\Psi)$ is given by an integral along the field line Ψ :

$$I(\Psi) = \int_{\Psi} \frac{d\theta}{B_\theta r \sin^2 \theta}. \quad (9)$$

Using equation (2), we can express the poloidal field B_θ in terms of the function $r(\Psi, \theta)$ as

$$B_\theta = -\frac{1}{r \sin \theta} \frac{\partial \Psi}{\partial r} = -\frac{1}{r \sin \theta} \left(\frac{\partial r}{\partial \Psi} \right)^{-1}. \quad (10)$$

Then,

$$I(\Psi) = - \int_{\theta_*}^{\pi/2} \frac{d\theta}{\sin \theta} \frac{\partial r(\Psi, \theta)}{\partial \Psi} \simeq - \frac{\partial}{\partial \Psi} \int_{\theta_*}^{\pi/2} \frac{d\theta}{\sin \theta} r(\Psi, \theta), \quad (11)$$

where we have neglected the dependence of θ_* (the angular position of the footpoint on the surface of the star) on Ψ . We can do this because, in the regime of interest to our present study, only a relatively small amount of twist resides near the disk and the star surfaces, while the dominant contribution to the integral $I(\Psi)$ and, hence, to the total twist $\Delta\Phi$ for a strongly expanded field line comes from the part of the field line near the apex, $\theta = \theta_{\text{ap}}$. This is justified by the property of the twist to propagate along the flux tube and concentrate in the region of the weakest field (see Parker 1979), which in our case coincides with the apex region.

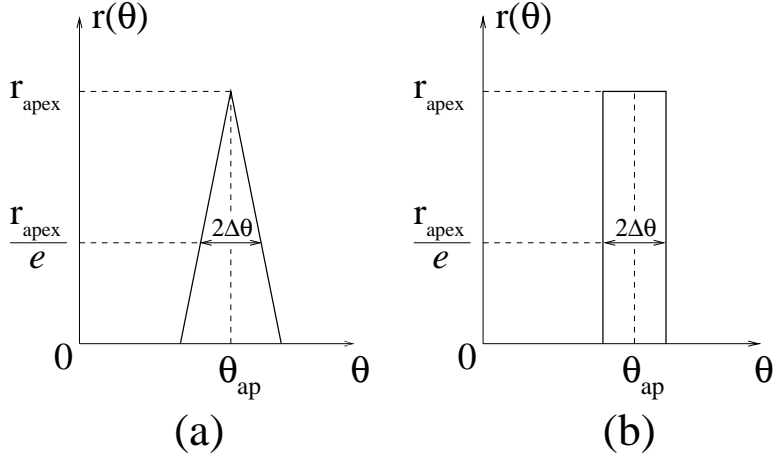


Fig. 4.— The two examples of field-line shapes used in the text to demonstrate the calculation of the parameter κ : (a) the triangular shape; (b) the rectangular shape.

Furthermore, we can see that, if a field line is expanded strongly, then we can write

$$\int_{\theta_*}^{\pi/2} \frac{d\theta}{\sin \theta} r(\Psi, \theta) \equiv \kappa \Delta\theta(\Psi) \frac{r_{\text{ap}}(\Psi)}{\sin \theta_{\text{ap}}}. \quad (12)$$

This equation serves as the definition of the parameter κ . Basically, this parameter describes the shape of the part of the field line near the apex [i.e., the part giving the main contribution to $I(\Psi)$], independent of the angular size $\Delta\theta(\Psi)$ and the radial size $r_{\text{ap}}(\Psi)$, which appear in equation (12) explicitly. If all the field lines keep the same basic functional form near the apex, while only the typical angular and radial scales differ, we can regard κ as being independent of Ψ . The validity of the assumption $\kappa = \text{const}$ is further strengthened by the observation that κ varies very little over a broad range of field-line shapes. To demonstrate this, we here explicitly calculate, as an illustration, the values of κ for two extremely different shapes, the triangular shape (Fig. 4a) and the rectangular shape (Fig. 4b).

In the triangular case, shown in Figure 4a, we have, using the fact that $\Delta\theta \ll 1$ and hence $\sin \theta \simeq \sin \theta_{\text{ap}} = \text{const}$,

$$\int \frac{d\theta}{\sin \theta} r(\Psi, \theta) \simeq \frac{1}{2} \frac{r_{\text{ap}}(\Psi)}{\sin \theta_{\text{ap}}} \frac{\Delta\theta}{1 - 1/e},$$

and so

$$\kappa_a = \frac{e/2}{e - 1} \simeq 1.3.$$

In the rectangular case, shown in Figure 4b, we again use $\Delta\theta \ll 1$ to approximate $\sin \theta \simeq \sin \theta_{\text{ap}} =$

const, and obtain

$$\int \frac{d\theta}{\sin \theta} r(\Psi, \theta) = \frac{r_{\text{ap}}(\Psi)}{\sin \theta_{\text{ap}}} \Delta \theta,$$

and so

$$\kappa_b = 1.0.$$

Thus, from now on, we shall assume that κ is constant.

Using equations (11) and (12) we can now write

$$I(\Psi) = -\frac{\kappa}{\sin \theta_{\text{ap}}} \frac{d}{d\Psi} \left(\Delta \theta r_{\text{ap}} \right). \quad (13)$$

Substituting this into equation (8), we get

$$F(\Psi) = -\frac{\Delta \Phi(\Psi)}{\kappa r_{\text{ap}}(\Psi)} \frac{\sin \theta_{\text{ap}}}{\Delta \theta(\Psi)} \frac{\Psi}{(d \log \Delta \theta / d \log \Psi) - S(\Psi)}, \quad (14)$$

where

$$S(\Psi) \equiv \left| \frac{d \log r_{\text{ap}}(\Psi)}{d \log \Psi} \right| = -\frac{\Psi}{r_{\text{ap}}} \frac{dr_{\text{ap}}}{d\Psi}. \quad (15)$$

4. The θ Force Balance

Consider the θ component of the force balance equation:

$$\begin{aligned} \frac{4\pi}{c} [\mathbf{j} \times \mathbf{B}]_{\theta} &= \frac{4\pi}{c} (j_{\phi} B_r - j_r B_{\phi}) \\ &= \frac{B_r}{r} \frac{\partial}{\partial r} (r B_{\theta}) - \frac{B_r}{r} \frac{\partial B_r}{\partial \theta} - \frac{B_{\phi}}{r \sin \theta} \frac{\partial}{\partial \theta} (\sin \theta B_{\phi}) = 0. \end{aligned} \quad (16)$$

Here, the first term represents the θ component of the magnetic tension force, and the second and the third terms represent the θ derivatives of the radial and the toroidal field pressures, respectively. Intuitively, it is clear that the first term must be small compared with the other two terms, because the primary force balance across the apex region should be between the toroidal field pressure at the apex and the radial field pressure outside the apex. The magnetic tension acts mainly in the radial direction while its θ component is small. The same conclusion can also be reached upon noticing that the first two terms in equation (16) come from the corresponding two terms in the expression for the toroidal current density, $j_{\phi} = (1/r)(\partial/\partial r)(r B_{\theta}) - (1/r)(\partial B_r/\partial \theta)$. It is intuitively clear that, in the configuration where the field lines are strongly elongated in the radial direction and the radial field changes its sign across the apex line over a very narrow region, the second term gives a much greater contribution to j_{ϕ} than the first term. In § 6, we shall come back to this conclusion

and make a more rigorous *a posteriori* check of its validity, but now we shall just neglect the first term in equation (16) and thus get

$$\frac{B_\phi}{\sin \theta} \frac{\partial}{\partial \theta} (B_\phi \sin \theta) + B_r \frac{\partial B_r}{\partial \theta} = 0. \quad (17)$$

Notice that B_ϕ changes on the angular scale $\Delta\theta \ll 1$, while $\sin \theta$ changes on the angular scale of order 1 rad. Therefore, we can neglect the variation of $\sin \theta$ with θ and write

$$\frac{\partial}{\partial \theta} (B_\phi^2 + B_r^2) = 0 \quad \Rightarrow \quad B_\phi^2 + B_r^2 = \text{const} \quad \text{at fixed } r. \quad (18)$$

At the apex $\theta = \theta_{\text{ap}}$, $B_r = 0$, while outside the apex region, $\theta > \theta_{\text{ap}} + \Delta\theta_2/2$, B_ϕ becomes small. Hence, we obtain (consistent with the intuitive explanation given above) the pressure balance between the toroidal field at the apex and the radial field pressure outside the apex:

$$\left| B_\phi(r_{\text{ap}}, \theta_{\text{ap}}) \right| = \left| B_r \left(r_{\text{ap}}, \theta > \theta_{\text{ap}} + \frac{\Delta\theta_2}{2} \right) \right| \quad (19)$$

The toroidal field $B_\phi(r_{\text{ap}}, \theta_{\text{ap}})$ is easily expressed in terms of $F(\Psi)$:

$$B_\phi(r_{\text{ap}}, \theta_{\text{ap}}) = \frac{F(\Psi)}{r_{\text{ap}}(\Psi) \sin \theta_{\text{ap}}}. \quad (20)$$

As for $B_r(r_{\text{ap}}, \theta > \theta_{\text{ap}} + \Delta\theta_2/2)$, we shall estimate it as follows. The total poloidal flux $\Delta\Psi$ through the interval $\theta \in [\theta_{\text{ap}} + \Delta\theta_2/2, \pi/2]$ per one radian in the toroidal direction at fixed $r = r_{\text{ap}}(\Psi)$ is equal to $\Delta\Psi = \Psi(r, \theta_{\text{ap}} + \Delta\theta_2/2) - \Psi(r, \pi/2)$. But, since we assume that $\Delta\theta_2 \ll 1$, we can approximate $\Psi(r_{\text{ap}}(\Psi), \theta_{\text{ap}} + \Delta\theta_2/2) \approx \Psi(r_{\text{ap}}(\Psi), \theta_{\text{ap}}) \equiv \Psi$. In addition, for strongly expanded field lines, $r_{\text{ap}}(\Psi) \gg r_0(\Psi)$, and hence $\Psi \gg \Psi[r_0 = r_{\text{ap}}(\Psi)]$ (where we take $\Psi = 0$ at infinity). Thus, we can evaluate $\Delta\Psi$ as $\Delta\Psi \approx \Psi$.

On the other hand, $\Delta\Psi$ can be estimated as

$$\Delta\Psi = -r_{\text{ap}}^2(\Psi) \int_{\theta_{\text{ap}} + \Delta\theta_2/2}^{\pi/2} B_r \sin \theta \, d\theta. \quad (21)$$

In the interval under consideration (i.e., $\theta \in [\theta_{\text{ap}} + \Delta\theta_2/2, \pi/2]$), B_r is roughly uniform, and so, using $\Delta\Psi \approx \Psi$, we can write

$$B_r \left(r_{\text{ap}}, \theta > \theta_{\text{ap}} + \frac{\Delta\theta_2}{2} \right) \simeq -\frac{a_1 \Psi}{r_{\text{ap}}^2(\Psi)} < 0, \quad (22)$$

where

$$a_1^{-1} \equiv \int_{\theta_{\text{ap}} + \Delta\theta_2/2}^{\pi/2} \sin \theta d\theta = \cos\left(\theta_{\text{ap}} + \frac{\Delta\theta_2}{2}\right) \simeq \cos \theta_{\text{ap}} \simeq 2 \quad (23)$$

is a constant.

Note that estimate (22) is consistent with the self-similar model, which would give (see §§ 2.1 and 2.3 of Uzdensky et al. 2002a)

$$B_r^{\text{self-similar}}\left(r_{\text{ap}}, \theta > \theta_{\text{ap}} + \frac{\Delta\theta_2}{2}\right) \simeq \frac{G'_0(\pi/2)}{G_{0,\text{max}} \sin \theta_{\text{ap}}} \frac{\Psi}{r_{\text{ap}}^2(\Psi)}. \quad (24)$$

Since the function $G_0(\theta)$ is roughly linear in the interval $[\theta_{\text{ap}} + \Delta\theta_2/2, \pi/2]$, we can write $G_{0,\text{max}} \simeq -G'_0(\pi/2)(\pi/2 - \theta_{\text{ap}})$, and so

$$B_r^{\text{self-similar}}\left(r_{\text{ap}}, \theta > \theta_{\text{ap}} + \frac{\Delta\theta_2}{2}\right) \simeq -\frac{\Psi}{r_{\text{ap}}^2(\Psi) \sin \theta_{\text{ap}}} \frac{1}{\pi/2 - \theta_{\text{ap}}} \simeq -\frac{a_1 \Psi}{r_{\text{ap}}^2(\Psi)}. \quad (25)$$

Thus, combining equations (19), (20), and (22), we get

$$F(\Psi) = a_1 \sin \theta_{\text{ap}} \frac{\Psi}{r_{\text{ap}}(\Psi)}. \quad (26)$$

Combining this with equation (14), we get

$$\frac{d \log \Delta\theta(\Psi)}{d \log \Psi} - S(\Psi) = -\frac{\Delta\Phi(\Psi)}{\kappa a_1 \Delta\theta(\Psi)}. \quad (27)$$

This equation presents a physically sound and adequate description of the system's behavior, with most of the uncertainties associated with its derivation being hidden in the constants κ and a_1 .

5. The Radial Force Balance

Consider now the radial force balance along the apex line $\theta = \theta_{\text{ap}}$. Physically, we have here a balance between the radial outward pressure of the toroidal field, the term on the right hand side, and the poloidal field tension, second term on the left hand side of the Grad-Shafranov equation (3). The first term on the left hand side, the poloidal field pressure, is small in our limit $\Delta\theta \ll 1$. The fact that this first term is much smaller than the second term can also be understood as the statement that, in the expression for the toroidal current density, $j_\phi = (1/r)(\partial/\partial r)(rB_\theta) - (1/r)(\partial B_r/\partial \theta)$, the first term is much smaller than the second term. Thus, we see that the criterion for validity of the assumption that the first term in equation (3) is much smaller than the second term coincides with the criterion for validity of a similar assumption we made when deriving equation (17) from equation (16). Thus, both these assumptions will be justified simultaneously in the next section.

So, we now have

$$\frac{\sin \theta_{\text{ap}}}{r_{\text{ap}}^2} \frac{\partial}{\partial \theta} \left(\frac{1}{\sin \theta} \frac{\partial \Psi}{\partial \theta} \right) \Big|_{\text{apex}} = -FF'(\Psi), . \quad (28)$$

(Note that our interpretation of the Grad–Shafranov equation only makes sense if the toroidal field pressure is directed outward, which corresponds to $dF^2/d\Psi > 0$).

Neglecting, as usual, the θ variation of $\sin \theta$ in comparison with that of the magnetic field quantities, we write

$$\frac{1}{r_{\text{ap}}^2} \frac{\partial^2 \Psi}{\partial \theta^2} \Big|_{\text{apex}} = -FF'(\Psi), . \quad (29)$$

We can estimate $\partial^2 \Psi / \partial \theta^2$ at $\theta = \theta_{\text{ap}}$ as

$$\frac{\partial^2 \Psi}{\partial \theta^2} \Big|_{\text{apex}} = a_2 \frac{(\partial \Psi / \partial \theta)|_{\theta_{\text{ap}} + \Delta \theta_2 / 2} - (\partial \Psi / \partial \theta)|_{\theta_{\text{ap}}}}{\Delta \theta_2 / 2} \Big|_{r=r_{\text{ap}}}, \quad (30)$$

where a_2 is another constant of order one.

At the apex $\partial \Psi / \partial \theta \equiv 0$ by definition, so

$$\frac{\partial^2 \Psi}{\partial \theta^2} \Big|_{\text{apex}} = \frac{2a_2}{\Delta \theta_2} \frac{\partial \Psi}{\partial \theta} \Big|_{\theta_{\text{ap}} + \Delta \theta_2 / 2} = \frac{2a_2}{\Delta \theta_2} r_{\text{ap}}^2 \sin \theta_{\text{ap}} B_r \left(r_{\text{ap}}, \theta = \theta_{\text{ap}} + \frac{\Delta \theta_2}{2} \right). \quad (31)$$

Using our estimate (22) for $B_r(r_{\text{ap}}, \theta = \theta_{\text{ap}} + \Delta \theta_2 / 2)$, we get

$$\frac{\partial^2 \Psi}{\partial \theta^2} \Big|_{\text{apex}} = -\frac{2a_1 a_2}{\Delta \theta_2} \Psi \sin \theta_{\text{ap}}. \quad (32)$$

Then, from equation (29),

$$FF'(\Psi) = \frac{2a_1 a_2}{\Delta \theta_2} \frac{\Psi}{r_{\text{ap}}^2}. \quad (33)$$

Thus we have obtained the following system of equations:

$$F(\Psi) = a_1 \sin \theta_{\text{ap}} \frac{\Psi}{r_{\text{ap}}(\Psi)}, \quad (34)$$

$$FF'(\Psi) = \frac{2a_1 a_2}{\Delta \theta_2} \frac{\Psi}{r_{\text{ap}}^2}, \quad (35)$$

$$\frac{d \log \Delta \theta(\Psi)}{d \log \Psi} - S(\Psi) = -\frac{\Delta \Phi(\Psi)}{\kappa a_1 \Delta \theta(\Psi)}. \quad (36)$$

We view this system as a system of three equations for three functions, $F(\Psi)$, $r_{\text{ap}}(\Psi)$, and $\Delta \theta(\Psi)$.

To simplify this system, we shall first use equation (34) to eliminate function $F(\Psi)$. We have

$$F'(\Psi) = \frac{a_1 \sin \theta_{\text{ap}}}{r_{\text{ap}}(\Psi)} \left[1 + S(\Psi) \right]. \quad (37)$$

Substituting this, together with equation (34), into equation (35), we get

$$\left[1 + S(\Psi) \right] \Delta\theta_2(\Psi) = \frac{2a_2}{a_1 \sin^2 \theta_{\text{ap}}} \equiv C^{-1} = \text{const} = O(1). \quad (38)$$

For example, for $a_1 = 1/2$, $a_2 = 1$, and $\sin \theta_{\text{ap}} \simeq 1$, we have $C \simeq 1/4$.

Now note that, because we are in the small- $\Delta\theta$ regime, from equation (38) it follows that

$$S(\Psi) \equiv \left| \frac{d \log r_{\text{ap}}}{d \log \Psi} \right| \gg 1. \quad (39)$$

Then equation (38) becomes

$$CS(\Psi)\Delta\theta_2(\Psi) = 1. \quad (40)$$

It is interesting to note that, since $S = -d \log r_{\text{ap}} / d \log \Psi$, then $\Psi(r, \theta_{\text{ap}}) \sim r^{-1/S}$, that is, $1/S$ represents a direct analog of the power exponent n in the self-similar models of VB94, Uzdensky et al. 2002a, Low & Lou (1990), and Wolfson (1995) (and the power exponent p in LBB94). Thus, the last equation can be interpreted as a statement that $n = 1/S \sim \Delta\theta_2 \rightarrow 0$ as a thin current layer forms, in agreement with LBB94 and Wolfson (1995). This shows that a current sheet formation is intrinsically related to the increase in S , and hence can be attributed to a growing difference in the expansion ratios of neighboring field lines with different twist angles, as discussed at the end of § 1.

6. Analysis and Interpretation of the Results

Thus we managed to reduce the problem to a system of two equations, namely, equation (40) and equation (36). The latter can be rewritten as

$$\frac{1}{S\Delta\theta_2} \frac{d\Delta\theta}{dx} - \frac{\Delta\theta}{\Delta\theta_2} = -u(x). \quad (41)$$

Here

$$x \equiv \log \Psi, \quad (42)$$

and

$$u(x) \equiv \frac{\Delta\Phi(x)}{\Delta\Phi_c}, \quad (43)$$

where

$$\Delta\Phi_c \equiv \frac{\kappa a_1}{C} = \frac{2\kappa a_2}{\sin^2 \theta_{\text{ap}}} = \text{const} = O(1) \quad (44)$$

is some critical twist angle. For example, for $\kappa = 1$, $a_2 = 1$, and $\sin \theta_{\text{ap}} \simeq 1$, we get $\Delta\Phi_c \simeq 2$ rad. As we shall see below, the behavior of the system below and above $\Delta\Phi_c$ greatly differs.

It is convenient to define a new independent variable

$$t = \log r_{\text{ap}}(\Psi). \quad (45)$$

Then,

$$S = -dt/dx, \quad (46)$$

and equation (41) becomes

$$\frac{\Delta\theta(t)}{\Delta\theta(t+1)} \left(1 - \frac{d \log \Delta\theta}{dt} \right) = u[x(t)]. \quad (47)$$

At this point we would like to pause in order to verify the validity of two steps in our program, namely the derivation of equations (17) and (28) in § 4 and § 5, respectively. The validity of both these steps was based on a single assumption that, at the apex $\theta = \theta_{\text{ap}}$ the first term in the expression for the toroidal current density, $j_\phi = (1/r)(\partial/\partial r)(rB_\theta) - (1/r)(\partial B_r/\partial\theta)$, is much smaller than the second term (in the limit $\Delta\theta \ll 1$ that we consider here). At this stage in our analysis we now have at our disposal all the tools necessary to estimate the magnitude of these two terms. Indeed, using equations (2), (39), and (40), the size of the first term can be evaluated as

$$\left| \frac{\partial}{\partial r} (rB_\theta) \right|_{\text{apex}} \sim \left| \frac{\partial^2 \Psi}{\partial r^2} \right|_{\text{apex}} \sim \frac{\Psi}{r_{\text{ap}}^2(\Psi)} \left[O\left(\frac{1}{S}\right) + O\left(\left| \frac{d\Delta\theta_2}{dt} \right| \right) \right] \ll \frac{\Psi}{r_{\text{ap}}^2(\Psi)}. \quad (48)$$

At the same time, using equations (1), and (32), the second term, $(1/r)(\partial B_r/\partial\theta)$, can be estimated at $\theta = \theta_{\text{ap}}$ as

$$\left| \frac{1}{r} \frac{\partial B_r}{\partial \theta} \right|_{\text{apex}} \sim \frac{1}{r^2} \left| \frac{\partial^2 \Psi}{\partial \theta^2} \right|_{\text{apex}} \sim \frac{\Psi}{r_{\text{ap}}^2(\Psi)} \frac{1}{\Delta\theta_2} \gg \frac{\Psi}{r_{\text{ap}}^2(\Psi)}. \quad (49)$$

Thus, we see that the approximation we used is indeed well justified in the small- $\Delta\theta$ limit.

We now turn to the application of our results to several particular situations.

6.1. The Constant- u Solution

The *non-local* nature of equation (47) makes it very difficult to analyze. The situation is complicated even further by the fact that the dependence $x(t)$ and, hence, the right hand side of equation (47) are not explicitly known. However, an exact solution of this equation can be found in the case of

a disk rotating as a solid body, $\Delta\Phi(\Psi) = \text{const.}$ This may be, in fact, a good approximation for the outer parts of a Keplerian disk, $r \gg r_{\text{co}}$ (where r_{co} is the corotation radius), where $\Delta\Omega(\Psi) = \Omega_{\text{disk}}(\Psi) - \Omega_* \approx -\Omega_* = \text{const.}$ In this *uniformly-rotating* disk model, one thus has $u(x) = \text{const.}$ The solution that satisfies the boundary condition $\Delta\theta(t_0) = \Delta\theta_0$ is

$$\Delta\theta(t) = \Delta\theta_0 e^{(1-\xi)(t-t_0)}, \quad (50)$$

and the constant ξ is uniquely determined by u via

$$u = \xi e^{(\xi-1)}. \quad (51)$$

Next, using equation (40), we find $S = S_0 \exp[(\xi - 1)(t - t_0)]$, where $S_0 \equiv S(t_0) = u/C\xi\Delta\theta_0$. Then, using equation (46), we can calculate $x(t)$,

$$x = x_0 + \frac{1}{\xi - 1} \frac{1}{S_0} \left(e^{(1-\xi)(t-t_0)} - 1 \right), \quad (52)$$

and thus determine $\Delta\theta$ as a function of the poloidal flux:

$$\Delta\theta(x) = \Delta\theta_0 + \frac{u}{C\xi}(\xi - 1)(x - x_0) = \Delta\theta_0 + \frac{\xi - 1}{C} e^{\xi-1} \log \frac{\Psi}{\Psi_0}. \quad (53)$$

For each u there is a unique solution ξ , such that $\xi(u > 1) > 1$ and $\xi(u < 1) < 1$. This means that, if $u > 1$ (that is, $\Delta\Phi > \Delta\Phi_c$), then $\Delta\theta$ decreases outward, and if $u < 1$ ($\Delta\Phi < \Delta\Phi_c$), then $\Delta\theta$ increases outward. The special case $u = 1$ corresponds to $\xi = 1$ and $\Delta\theta = \text{const}$ and thus describes the approach to the singularity $\Delta\Phi_c$ in the self-similar case discussed by VB94 and Uzdensky et al. (2002a).

Notice that in the case $u < 1$ ($\xi < 1$), $\Delta\theta$ increases outward (with decreasing Ψ) until our model's main assumption $\Delta\theta \ll 1$ breaks down. This condition defines the outer boundary Ψ_{min} of applicability of the present model, which can be estimated roughly as the value of Ψ for which $\Delta\theta \simeq 1$:

$$\Psi_{\text{min}}(\xi) \simeq \Psi_0 \exp \left[-\frac{C}{1-\xi} e^{1-\xi} \right]. \quad (54)$$

We see that the range of validity of our model widens (Ψ_{min} decreases) as $\xi \rightarrow 1$.

In the opposite case $u > 1$ ($\xi > 1$) there exists a certain critical field line,

$$\Psi_c = \Psi_0 \exp \left[-\frac{C\Delta\theta_0}{\xi - 1} e^{1-\xi} \right], \quad (55)$$

on which $\Delta\theta$ vanishes while r_{ap} becomes equal to infinity. If u (and hence ξ) just barely exceeds 1, then this point is very far away: $\Psi_c \ll \Psi_0$ and $r_0(\Psi_c) \gg r_0(\Psi_0)$. As u and ξ increase, Ψ_c also increases and the critical field line moves inward.

We interpret the vanishing of $\Delta\theta(\Psi_c)$ as a partial field-line opening, with Ψ_c marking the boundary between open and closed field lines. Our model describes only closed field lines and thus is valid only for $\Psi > \Psi_c$. For any given field line $\Psi > \Psi_c$, $r_{\text{ap}}(\Psi)$ is still finite, and, since $r_{\text{ap}}(\Psi_c) = \infty$, the field line $\hat{\Psi}$ with $r_{\text{ap}}(\hat{\Psi}) = er_{\text{ap}}(\Psi)$ still lies between Ψ and Ψ_c . We can see then that the analysis given in the previous sections will still be valid for any field line $\Psi > \Psi_c$, no matter how close to Ψ_c . For open field lines, $\Psi < \Psi_c$, our treatment is, of course, no longer valid. However, such an elaborate analysis is not needed for these field lines because their physics is very simple: the open field ($\Psi < \Psi_c$) is potential, $F(\Psi) \equiv 0$, and mostly radial.

We would like to remark that expression (53) describes the behavior of the *angular width* of the current concentration region as a function of Ψ . We can also see whether the *physical width* of this region (which probably is of greater interest, as far as reconnection is concerned) decreases as $\Delta\theta \rightarrow 0$. From equation (52) we have

$$\frac{r_{\text{ap}}(x)}{r_{\text{ap}}(x_0)} = [S_0(\xi - 1)(x - x_0) + 1]^{\frac{1}{1-\xi}}, \quad (56)$$

and so

$$r_{\text{ap}}(\Psi) \Delta\theta(\Psi) \propto [\Delta\theta(\Psi)]^{\frac{2-\xi}{1-\xi}}. \quad (57)$$

We see that $r_{\text{ap}}\Delta\theta \rightarrow 0$ with $\Delta\theta$ if $\xi > 2$, i.e., if $u > 2e \approx 5.4$. Thus, we envision the following scenario. As the twist is increased beyond $u = 1$, there will be a line Ψ_c beyond which the field will be open: $r_{\text{ap}}(\Psi \rightarrow \Psi_c) \rightarrow \infty$. As the twist is increased even further, more and more flux becomes open. At the same time, as u is increased beyond $2e$, then, according to the power law (57), not only the angular, but also the actual physical width of the current concentration region, $r_{\text{ap}}\Delta\theta$, shrinks to zero as one takes the limit $\Psi \rightarrow \Psi_c$. This suggests that increasing the twist angle well above the critical value can not only result in a greater amount of open flux, but also can lead to a narrower current layer, thus facilitating magnetic reconnection.

We would like to emphasize that, while our analysis predicts a finite-time partial field opening, it does not, strictly speaking, predict a finite-time current-sheet formation in a true sense. Indeed, at any given $\Delta\Phi > \Delta\Phi_c$, and for any given still-closed field line $\Psi > \Psi_c(\Delta\Phi)$, the current concentration region has a non-zero angular thickness $\Delta\theta(\Psi, t)$ (which, however, tends to zero as $\Psi \rightarrow \Psi_c$). If one fixes a field line Ψ , and monitors how the angular thickness $\Delta\theta(\Psi, t)$ changes with time, then one finds that it does indeed go to zero in finite time at the moment of opening of this field line. If, however, one looks at any given *finite radius* r (instead of fixing a field line Ψ), then the situation is very different. Since $r_{\text{ap}}(\Psi_c) = \infty$, there is always a closed field line $\Psi > \Psi_c$ with $r_{\text{ap}}(\Psi) = r$; thus, the angular thickness $\Delta\theta(r, t)$ stays finite at the moment of first field-line opening (when $\Delta\Phi = \Delta\Phi_c$). As the twisting continues, $\Delta\theta(r, t)$ will probably decrease and may in fact go to zero asymptotically as $t \rightarrow \infty$. Thus, one may say that even though one has a finite-time partial field-line opening, there is no true finite-time current sheet formation. This is indeed a very important distinction. Of course, on a practical note, what is important here is the fact that the current layer

becomes very thin: at some point during the thinning process finite resistivity may come into play, leading to field-line reconnection.

Finally, we need to point out that, when partial field opening takes place, some parts of an opening field line move very rapidly (e.g., the velocity of the apex approaches infinity at the point of opening). We have to make it clear that these infinite velocities are an artifact of the equilibrium assumption. They should be understood only in the sense that they become very large compared with the footpoint rotation velocity. In reality, the expansion velocity will be limited, most likely, by finite inertia of the plasma, i.e., by the Alfvén speed. Another concern is the assumption that the suggested sequence of partially-open field configurations is continuous. It is actually not completely clear whether this always has to be so. In reality, it may be possible that, upon reaching a critical twist, a quasi-static evolution along a sequence of force-free fields will end abruptly by opening up a finite portion of the flux.

6.2. Solution in the vicinity of $\Delta\Phi_c$

Another important advance in our understanding of equation (47) can be made in a situation where $\Delta\Phi(\Psi)$ is nonuniform and passes through the critical twist angle $\Delta\Phi_c$ (for example, as one moves outward, i.e., as Ψ is decreased).

Let us consider a close vicinity of the point $x_0 \equiv \log \Psi_0$ where $u(x_0) = 1$. In this region we can Taylor-expand $u(x)$ and keep only the linear term:

$$u(x) = 1 - \eta(x - x_0), \quad \text{where } \eta = -\frac{du}{dx}(x_0) > 0. \quad (58)$$

Let us define two functions,

$$\epsilon(t) \equiv \frac{\Delta\theta(t+1) - \Delta\theta(t)}{\Delta\theta(t)}, \quad (59)$$

and

$$\sigma(t) \equiv \frac{d \log \Delta\theta(t)}{dt}, \quad (60)$$

and consider a region around $t_0 = t(x_0)$ corresponding to a close vicinity of x_0 , such that $|u-1| \ll 1$ within this region. We anticipate that $\Delta\theta$ varies relatively little so that $|\epsilon(t)| \ll 1$ everywhere in this region.

Then equation (47) becomes

$$(1 - \epsilon)(1 - \sigma) = u \approx 1, \quad (61)$$

and therefore $|\sigma(t)| \ll 1$, which gives us a relationship between $\epsilon(t)$ and $\sigma(t)$:

$$\epsilon(t) + \sigma(t) = 1 - u(t) \ll 1. \quad (62)$$

A second relationship follows from the definitions of $\epsilon(t)$ and $\sigma(t)$:

$$\epsilon(t) \simeq \int_t^{t+1} \sigma(\hat{t}) d\hat{t}, \quad (63)$$

where we have neglected higher-order corrections in $\sigma(t)$. Using this expression we can differentiate equation (62) and get

$$\sigma'(t) + \sigma(t+1) - \sigma(t) = -u'(t), \quad (64)$$

where prime denotes the derivative with respect to t .

Now let us Taylor-expand $\sigma(t+1)$ around the point t and keep only the first two terms:

$$\sigma(t+1) \approx \sigma(t) + \sigma'(t). \quad (65)$$

Then we can write

$$\sigma'(t) = -\frac{u'(t)}{2}. \quad (66)$$

We now need to make a little digression in order to discuss the validity of this step, that is of keeping only the first two terms in the expansion of $\sigma(t+1)$. In particular, we need to verify that we can safely neglect the next term in the Taylor expansion, $0.5 \sigma''(t)$. This term needs to be compared with the last term that we kept in the expansion, that is with $\sigma'(t)$, which, according to equation (66), can be rewritten as

$$\sigma'(t) = -\frac{u'(t)}{2} = \frac{1}{2S} \frac{du(x)}{dx} = \frac{C}{2} \frac{du(x)}{dx} \Delta\theta(t+1), \quad (67)$$

where we made use of equations (46) and (40). At the same time, the first neglected term is

$$\frac{\sigma''(t)}{2} = -\frac{C^2}{4} \frac{d^2u(x)}{dx^2} \Delta\theta^2(t+1) + \frac{C}{4} \frac{du(x)}{dx} \Delta\theta(t+1) \sigma(t+1),$$

where we again used equations (40) and (46), as well as equation (60). The second term in this expression is manifestly much smaller than (67) because we here are considering a region where $|\sigma(t)| \ll 1$. Thus we see that our approximation (65) is valid if

$$\left| \frac{du(x)}{dx} \right| \simeq \eta \gg \left| \frac{d^2u(x)}{dx^2} \right| \Delta\theta(t+1). \quad (68)$$

The function $u(x)$ is the prescribed twist angle as a function of flux; generally, it varies on a scale that is finite in Ψ and, hence, in x . This means that both du/dx and d^2u/dx^2 are of order 1; therefore, since we work in the regime $\Delta\theta \ll 1$, the above condition is easily satisfied and thus our truncation of the Taylor expansion (65) is valid.

We now continue with our analysis. Since we consider a region where $\Delta\theta$ is almost constant, we can, to the lowest order in σ , substitute $\Delta\theta(t+1)$ in equation (67) by $\Delta\theta_0 \equiv \Delta\theta(t_0)$, where t_0 is defined

by $x(t_0) = x_0$. In a similar vain, du/dx also varies very little in the region under consideration, so, using equation (58) we can substitute it by $-\eta$. Then we can integrate equation (67) to get

$$\sigma(t) = \sigma_0 - \frac{C\eta}{2}\Delta\theta_0(t - t_0) + O(\sigma^2), \quad (69)$$

where $\sigma_0 \equiv \sigma(t_0)$.

Combining this expression with the definition of $\sigma(t)$, we get the following expression for $\Delta\theta(t)$:

$$\begin{aligned} \Delta\theta(t) &= \Delta\theta_0 \exp\left[\sigma_0(t - t_0)\right] \cdot \exp\left[-\frac{C\eta}{4}\Delta\theta_0(t - t_0)^2\right] \\ &\simeq \Delta\theta_0 \left(1 + \sigma_0(t - t_0) - \frac{C\eta}{4}\Delta\theta_0(t - t_0)^2\right). \end{aligned} \quad (70)$$

Then, from equation (63) it follows that

$$\epsilon(t) = \sigma_0 - \frac{C\eta}{4}\Delta\theta_0[1 + 2(t - t_0)], \quad (71)$$

and from equation (62) we get

$$\sigma_0 \equiv \sigma(t_0) = \frac{C\eta}{8}\Delta\theta_0 > 0. \quad (72)$$

Thus, we can write

$$\Delta\theta(t) = \Delta\theta_0 \left[1 + \sigma_0(t - t_0)[1 - 2(t - t_0)]\right]. \quad (73)$$

We see that $\Delta\theta(t)$ behaves regularly at $t = t_0$; for $t > t_0$, it first increases, reaches a maximum at $t = t_0 + 1/4$ (i.e., $x - x_0 = -C\Delta\theta_0/4 \ll 1$), and then starts to decrease. If $u > 1$ for all $x < x_0$, then, guided by our constant- u solution, we can predict that $\Delta\theta$ at some point will reach zero, implying a partial field-line opening.

6.3. Locally enhanced twist

As a last example, we present the results of numerical solution of the system (47)–(46) for the case of a locally enhanced $u(x)$.

We consider an interval $x \in [x_{\text{out}}, x_{\text{in}}]$ corresponding to $\Psi \in [\Psi_{\text{out}}, \Psi_{\text{in}}]$. In order to be able to make a connection with the constant- u analytical solution, we take the function $u(x)$ to consist of three pieces (see Figure 5):

$$u(x) = u_0 < 1, x_{\text{out}} \leq x \leq x_1;$$

$$u(x) = u_1 > 1, x_1 < x < x_2;$$

and

$$u(x) = u_0, x_2 \leq x \leq x_{\text{in}}.$$

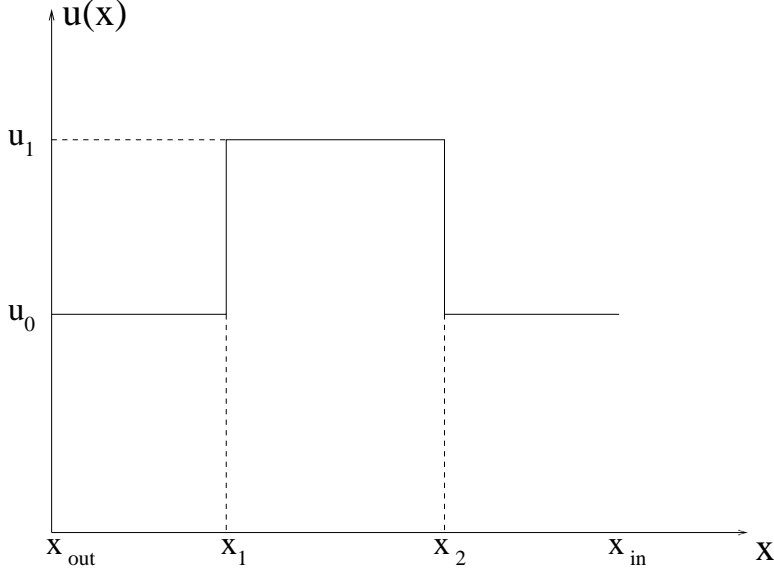


Fig. 5.— The $u(x)$ profile investigated in § 6.3.

Here, $u_0 = \text{const} < 1$ is some background value, which we keep fixed, and $\Delta u = u_1 - u_0 = \text{const}$ is the localized enhancement. We study a family of solutions of the system (47)–(46) with a fixed value of u_0 , $u_0 = 0.655..$ [which corresponds to $\xi_0 \equiv \xi(u_0) = 0.8$], but with several different values of u_1 . We start with $u_1 = 1.2$, and then gradually increase it until the sequence terminates at $u_1 \simeq 1.8$. In order for us to be able to make a meaningful comparison of the solutions with different values of u_1 , we fix the value of $\Delta\theta$ on the innermost field line, $\Delta\theta(x_{\text{in}}) = \Delta\theta_0$.

Now, based on our experience with constant- u solutions, we can naively expect the resulting function $\Delta\theta(x)$ to be roughly a piece-wise linear function, with $\Delta\theta(x)$ decreasing linearly in the intervals $x_{\text{out}} < x < x_1$ and $x_2 < x < x_{\text{in}}$ [with the slope $u_0(\xi_0 - 1)/C\xi_0$], and increasing linearly in the interval $x_1 < x < x_2$ [with the slope $u_1(\xi_1 - 1)/C\xi_1$, where $\xi_1 \equiv \xi(u_1) > 1$]. We thus expect $\Delta\theta$ to have a maximum at x_2 , $\Delta\theta_{\text{max}}^{\text{est}} = \Delta\theta(x_2) = \Delta\theta_0 + u_0(\xi_0 - 1)(x_2 - x_{\text{in}})/C\xi_0$, and a minimum at x_1 , $\Delta\theta_{\text{min}}^{\text{est}} = \Delta\theta(x_1) = \Delta\theta_{\text{max}}^{\text{est}} - u_1(\xi_1 - 1)(x_2 - x_1)/C\xi_1$.

Note that, when u_1 reaches a certain value $u_{1,\text{max}} > 1$ [and, correspondingly, $\xi_{1,\text{max}} \equiv \xi(u_{1,\text{max}}) > 1$] such that

$$(\xi_{1,\text{max}} - 1) \exp(\xi_{1,\text{max}} - 1) = \frac{C\Delta\theta_{\text{max}}}{x_2 - x_1}, \quad (74)$$

then $\Delta\theta_{\text{min}}^{\text{est}}$ becomes zero. We interpret this as the point in the sequence of equilibria at which a *partial field-line opening* occurs at $\Psi = \Psi_1$. Note that $u_{1,\text{max}}$, i.e., the maximum allowable value of u_1 , depends inversely on the size $(x_1 - x_2)$ of the enhanced-twist region. We thus see that, if only a portion of field lines (those between Ψ_1 and Ψ_2) are participating in twisting and expansion, then the thinning of the current layer, and the corresponding partial field-line opening, is achieved

not at $u = 1$, but at a somewhat higher value.

When performing the actual computation, we advance along t from t_{out} (corresponding to the outermost field line Ψ_{out}) inward. We first pick a guess for the initial value of $\Delta\theta$ at the outer boundary, $\Delta\theta_{\text{out}}$, and then use our const- u solution to prescribe the function $\Delta\theta(t)$ and hence $x(t)$ in the *initial interval* of unit length, $t \in [t_{\text{out}} - 1, t_{\text{out}}]$. After that, we proceed to integrate the two differential equations:

$$\frac{d\Delta\theta}{dt} = \Delta\theta(t) - u[x(t)]\Delta\theta(t+1), \quad (75)$$

$$\frac{dx}{dt} = -\frac{1}{S(t)} = -C\Delta\theta(t+1). \quad (76)$$

We stop when the innermost field line of the domain, $x = x_{\text{in}}$, $\Psi = \Psi_{\text{in}}$, is reached and compare the computed value of $\Delta\theta$ at this point with the prescribed value $\Delta\theta_{\text{in}} = \Delta\theta_0$. We then iterate with respect to $\Delta\theta_{\text{out}}$, i.e., we change $\Delta\theta_{\text{out}}$ and repeat the procedure until $\Delta\theta(x_{\text{in}})$ finds itself within a small vicinity (which we usually take to be 1%) of the desired value $\Delta\theta_0$.

In Figure 6 we present the results of our computations for $\Delta\theta_0 = 0.3$, $x_{\text{out}} = 0.0$, $x_1 = 0.5$, $x_2 = 1.5$, $x_{\text{in}} = 2.0$, $C = 1$, $u_0 = 0.655$, and u_1 between 1.2 and 1.8. We indeed see that the obtained solutions $\Delta\theta(x)$ are in good agreement with the analytically-predicted picture described above. In particular, we find $\Delta\theta_{\text{max}} \simeq 0.43$, and $u_{1,\text{max}} \simeq 1.8$. This is very close to the naive prediction (74), which gives $\Delta\theta_{\text{max}} = 0.382$, $\xi_{1,\text{max}} = 1.287$, and $u_{1,\text{max}}^{\text{est}} = 1.71$ for the set of parameters that we chose. And, if we use the actual value $\Delta\theta_{\text{max}} = 0.43$ in equation (74), we then get $\xi_{1,\text{max}} = 1.314$, and $u_{1,\text{max}}^{\text{est}} = 1.80$.

At the same time we observe that, as $u_{1,\text{max}}$ is approached, the apexes of the field lines move out to infinity explosively fast, signaling a partial field-line opening at a finite twist. This opening can be illustrated by the behavior of the natural logarithm of the ratio of r_{ap} of the outermost field line to r_{ap} of the innermost field line, i.e., by $t_{\text{out}} - t_{\text{in}} \equiv \log[r_{\text{ap}}(\Psi_{\text{out}})/r_{\text{ap}}(\Psi_{\text{in}})]$. Figure 7 shows this ratio as a function of u_1 . We thus see an unambiguous evidence that the thinning of the current layer occurs simultaneously with the partial field-line opening, in accord with our expectations discussed in § 1.

7. Conclusions

In this paper we addressed the issue of the formation of thin current structures in the magnetosphere of an accretion disk in response to the field-line twisting. We presented a simple analytical model that illustrates the asymptotic behavior of a force-free axisymmetric magnetic field above a thin conducting disk in the limit when such structures are about to form. We showed that there exist a finite critical twist angle, $\Delta\Phi_c$, such that the expansion of the poloidal field lines

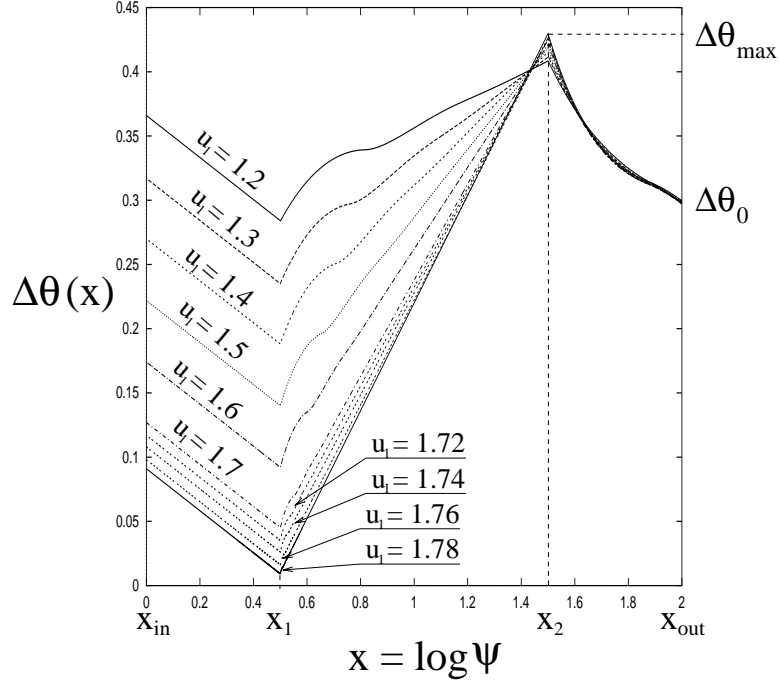


Fig. 6.— Angular thickness $\Delta\theta$ as a function of $x \equiv \log \Psi$ for a range of values of u_1 between $u_1 = 1.2$ and $u_1 = 1.8$.

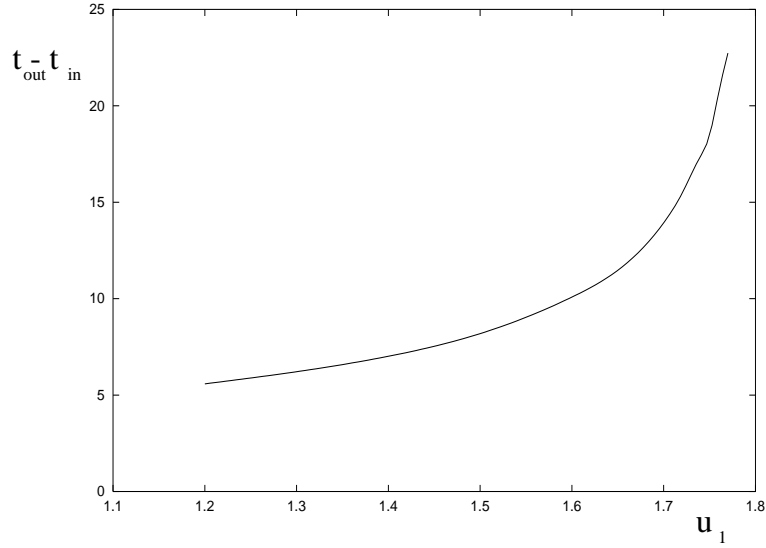


Fig. 7.— Natural logarithm of the ratio of r_{ap} of the outermost field line to r_{ap} of the innermost field line, $t_{\text{out}} - t_{\text{in}} \equiv \log[r_{\text{ap}}(\Psi_{\text{out}})/r_{\text{ap}}(\Psi_{\text{in}})]$, as a function of the twist u_1 .

accelerates dramatically as $\Delta\Phi_c$ is exceeded. At the same time, in the case of a locally-enhanced twist,⁶ a radially-extended thin conical current layer forms. Simultaneously, the field configuration approaches a partially-open state in finite time, with the apexes of a portion of the field lines going out to infinity.

The presence of a thin current sheet is usually considered a pre-requisite for reconnection of magnetic field lines. It is also believed that reconnection will occur whenever a thin current layer is formed. We therefore believe that magnetic field lines that have become effectively open as a result of their twist-driven inflation may subsequently reconnect via the thin current layer that has been formed simultaneously with their opening-up. This conclusion leads to important consequences regarding the time evolution of magnetospheres of magnetically-linked star–disk systems. In particular, we believe that, once the magnetic link between the star and the disk is broken by the partial field-line opening, a current layer will form along the separatrix between the stellar field lines and the disk field lines and, as a result, the link will be re-established through reconnection of these field lines. Subsequently, if reconnection process is sufficiently fast, the field lines will contract to a less-stressed configuration allowing a new cycle of twisting, inflation, opening, and reconnection to begin, as was suggested by Aly & Kijpers (1990) and by VB94 and illustrated in numerical simulations by Goodson et al. (1999). This quasi-periodic scenario is characterized by very rich physics with non-steady and violent behavior, perhaps not too different from that of the solar corona (e.g., Low 2001). It can provide avenues for understanding such phenomena as disk winds, time-variable, knotted jets, episodes of rapid accretion, and variable accretion torque on the central star.

One should note, however, that a true opening will be preceded by the plasma inertia becoming important. The inertial effects will tend to retard the expansion, since the pressure of the toroidal field pressure will have to work not only against the poloidal field tension, but also against the plasma inertia. Hence the inertial effects will in effect act against the toroidal field removal and will not help to form a current sheet. At some point during the expansion they will need to be taken into account and, even in the absence of reconnection, a true finite-time field opening will not happen. Instead, one will have a transition from the force-free regime into the inertial regime (wind regime), which would require solving the full set of MHD equations, although probably under some simplifying assumptions.

I am very grateful to Stanislav Boldyrev, Arie Königl, and Bob Rosner for very useful discussions and comments. I am also grateful to the anonymous referee for his or her deep and insightful criticism that was very beneficial for the paper. I would also like to acknowledge the support by the ASCI/Alliances Center for Astrophysical Thermonuclear Flashes at the University of Chicago

⁶An important example of the locally-enhanced-twist case is a Keplerian disk whose inner edge is significantly closer to the central star than the corotation radius. In particular, if $r_{\text{inner}} < 0.63 r_{\text{co}}$, then the relative star–disk angular velocity, $\Delta\Omega(r) = \Omega_{\text{disk}}(r) - \Omega_*$, reaches higher values in the localized inner region ($r_{\text{inner}} < r < r_{\text{co}}$) than at large distances ($r > r_{\text{co}}$).

under DOE subcontract B341495 and by the NSF grant NSF-PHY99-07949.

REFERENCES

- Aly, J. J. 1984, *ApJ*, 283, 349
- Aly, J. J., & Kuijpers, J. 1990, *A&A*, 227, 473
- Aly, J. J. 1995, *ApJ*, 439, L63
- Barnes, C. W., & Sturrock, P. A. 1972, *ApJ*, 174, 659
- Bertout, C., Basri, G., & Bouvier, J. 1988, *ApJ*, 330, 350
- Ghosh, P., & Lamb, F. K. 1978, *ApJ*, 223, L83 (GL)
- Ghosh, P., & Lamb, F. K. 1979a, *ApJ*, 232, 259 (GL)
- Ghosh, P., & Lamb, F. K. 1979b, *ApJ*, 234, 296 (GL)
- Goodson, A. P., Winglee, R. M., & Böhm, K.-H. 1997, *ApJ*, 489, 199
- Goodson, A. P., Böhm, K.-H., & Winglee, R. M. 1999, *ApJ*, 524, 142
- Königl, A. 1991, *ApJ*, 370, L39
- Lamb, F. K. 1989, in *Timing Neutron Stars*, ed. H. Ögelman & E. P. J. van den Heuvel (Dordrecht: Kluwer), 649
- Lovelace, R. V. E., Romanova, M. M., & Bisnovatyi-Kogan, G. S. 1995, *MNRAS*, 275, 244
- Low, B. C. 1986, *ApJ*, 307, 205
- Low, B. C., & Lou, Y. Q. 1990, *ApJ*, 352, 343
- Low, B. C. 1990, *ARA&A*, 28, 491
- Low, B. C. 2001, *JGR*, 106, 25141
- Lynden-Bell, D., & Boily, C. 1994, *MNRAS*, 267, 146 (LBB94)
- Mikić, Z., & Linker, J. A. 1994, *ApJ*, 430, 898
- Parker, E. N. 1979, *Cosmical Magnetic Fields* (Oxford: Oxford Univ. Press)
- Patterson, J. 1994, *PASP*, 106, 209

- Roumeliotis, G., Sturrock, P. A., & Antiochos S. K. 1994; ApJ, 423, 847
- Uzdensky, D. A., Königl, A., & Litwin, C. 2002a, ApJ, 565, 1191; also astro-ph/0011283
- Uzdensky, D. A., Königl, A., & Litwin, C. 2002b, ApJ, 565, 1205; also astro-ph/0011283
- van Ballegooijen, A. A. 1994, Space Sci. Rev., 68, 299 (VB94)
- Wang, Y.-M. 1987, A&A, 183, 257
- Wolfson, R., & Low, B. C. 1992, ApJ, 391, 353
- Wolfson, R. 1995, ApJ, 443, 810